PROCEEDINGS OF THE IV INTERNATIONAL CONFERENCE/HIGH TEMPERATURE CAPILLARITY

JOURNAL OF MATERIALS SCIENCE **40** (2005) 2431 – 2435

Nucleation of crystals in deeply undercooled alloy melts

M. PALUMBO, C. PAPANDREA, L. BATTEZZATI*
Dipartimento di Chimica I.F.M., Centro di Eccellenza NIS Superfici ed Interfasi Nanostrutturate, Università di Torino, via Giuria 9, 10125 Torino, Italy
E-mail: livio.battezzati@unito.it

The CALPHAD approach coupled with modelling of solid-liquid interfacial energy has been used to calculate the driving force for nucleation in undercooled melts. Thermodynamic parameters needed in nucleation have been evaluated using simplified formulae or numerical methods from assessed phase diagrams. Various models for the interfacial energy and its temperature dependence have been used. Phase selection on solidification and devitrification of glasses as well as the range of amorphous phase formation have been predicted in the Al-Ce and Fe-B systems and compared with those experimentally determined. Furthermore, the formation of quasicrystals in the Al-Mn and the competition with other compounds has been investigated.

1. Introduction

Liquid alloys can often be deeply undercooled before crystallisation. In the undercooled regime metastable crystal phases may nucleate instead of equilibrium ones with a consequent modification of the solidification path. As a limiting case, a glass is produced at the glass transition temperature avoiding crystal nucleation. According to the classical theory [1], the homogeneous nucleation frequency I_V is given by

$$I_V = K(T) \cdot \exp(-\Delta G^*/RT) \quad (1)$$

where $K(T)$ is a function of atomic mobility, R is the gas constant, T is the temperature and

$$\Delta G^* = \frac{16}{3}\pi \frac{\gamma_{SL}^3}{(\Delta\mu)^2} \quad (2)$$

is the driving force for nucleation of a spherical crystal. $\Delta\mu$ is the chemical potential difference between liquid and crystal phases and γ_{SL} is the interfacial energy between crystal and melt. $\Delta\mu$ is only rarely accessible to direct measurements, but can be obtained from empirical formulae or computer calculation of phase diagrams (CALPHAD) [2, 3]. Analogously, γ_{SL} is known for elements at the melting point [4] but must be modelled for alloys and compounds.

The search for new compositions of multicomponent metallic glasses [5–6] can benefit from the evaluation of driving forces for nucleation of crystal phases, as shown recently for Al-based alloys [7]. Among other metastable phases, the nucleation of quasicrystals is specially relevant because of the closeness of short range order in the solid and the melt [8]. This can provide a test for models of γ_{SL}.

Aim of this work is the calculation of the driving force for nucleation of Al, Fe and compounds in simple glass-forming systems (Al-Ce and Fe-B) and of the icosahedral phase in Al-Mn, where it has first been discovered in 1984 [9]. Assessments of the phase diagrams are reported in the literature ([10] for Fe-B, [2] for Al-Ce, [11] for Al-Mn). They have been used to provide the thermodynamic basis for calculations. Extrapolations in the undercooling regime of the optimised liquid free energy functions are required and their accuracy was checked by comparing the computed difference in enthalpy between liquid and crystal phases with the heat of crystallisation available from experiments [12].

γ_{SL} is known experimentally for a number of elements and for a few binary compositions and compounds at their melting point, often with large uncertainties [13, 14]. In the undercooling regime γ_{SL} is not an equilibrium quantity, it becomes an operative parameter expressing the work needed for crystal nucleation. The interfacial energy has been obtained from empirical formulae or models of the liquid-crystal interface. The results of calculations are used to predict the sequence of phases obtained in solidification of melts or devitrification of glasses.

2. Modelling

It has been chosen to consider nucleation as homogenous although it is recognised that in most instances heterogeneous nucleation would occur. However, the "shape factor" in Equation 2 causing reduction of the value of ΔG^*, depends on every single

*Author to whom all correspondence should be addressed.

heterogeneity and is generally unknown. Therefore calculations would be difficult to perform and impossible to compare. The validity of the results will be assessed *a posteriori* from comparison with experiments.

The composition of the most probable nucleus is different from that of the matrix. It is defined at constant temperature by applying the "parallel tangent construction" [15, 16] to the liquid free energy curve at the alloy composition and to the solid free energy curve. If the difference in the chemical potential of an element in the two phases is noted by $\Delta\mu$, a simple expression for an element nucleating in a regular liquid solution is [15]:

$$\Delta\mu = (T_l - T)\left(\Delta S^{\mathrm{A}}_{\mathrm{melt}} - R\ln x_A\right) \qquad (3)$$

where T_l is the liquidus temperature, $\Delta S^{\mathrm{A}}_{\mathrm{melt}}$ and x_A are the entropy of melting and the alloy mole fraction of component A, respectively.

The Gibbs free energy of glass-forming melts deviates usually from regularity because of the temperature dependence of thermodynamic quantities caused by the substantial excess specific heat [17, 18] so Equation 3 is no more suited. A reliable description of the thermodynamic functions can be obtained by means of the CALPHAD approach for calculation of phase equilibria. The method uses a multiparametric fitting procedure of experimental data to provide optimised thermodynamic functions. In glass-forming system, the amorphous phase and the liquid-glass transition must be modelled. Furthermore, metastable compounds must be included in the simulation if they compete in stability with the glass. This approach has been applied to the Fe-B and Al-Ce systems [2, 10, 12] using the ThermoCalc software [19].

The crystal-liquid interfacial energy of metals scales with the enthalpy of melting as shown by the early data of Turnbull [20]:

$$\gamma_{\mathrm{SL}} = \alpha \cdot \Delta H_{\mathrm{m}} / V_{\mathrm{m}}^{2/3} N_{\mathrm{a}}^{1/3} \qquad (4)$$

where α is an empirical constant taken as 0.44, V_{m} is the molar volume of the solid and N_{a} is the Avogadro's constant. Droplet undercooling experiments of pure metals [21, 22] confirmed this α value. Non structural models for the temperature dependence of γ_{SL} have been proposed using the "diffuse interface" approach [23, 24]. A proportionality between the work needed to create the crystal-melt interface and the temperature was derived. The following formula fits well the computed γ_{SL} in the undercooling regime down to 1/2 T_{m} (T_{m} is the melting point):

$$\gamma_{\mathrm{SL}}(T)/\gamma_{\mathrm{SL}}(T_{\mathrm{m}}) = 0.48 + 0.52 \cdot (T/T_{\mathrm{m}}) \qquad (5)$$

where $\gamma_{\mathrm{SL}}(T_m)$ is the crystal-liquid interfacial energy at the melting point.

A simpler non-structural model [16, 25], where a sharp crystal/melt interface is assumed, has yielded the following expression:

$$\gamma_{\mathrm{SL}}(T) = [0.24 + 0.29 \cdot (T/T_{\mathrm{m}})]\Delta H_{\mathrm{m}} / V_{\mathrm{m}}^{2/3} N_{\mathrm{a}}^{1/3} \qquad (6)$$

For compounds the lack of experimental data is nearly complete. Considerations on crystal plane symmetry and occupancy suggest that non structural models are not suitable to describe a monolayer interface between the crystalline compound and the melt. In a recent paper [14] a structural approach has been introduced to model the surface of several Al-transition metal compounds showing that Equation 4 can still be applied though using different values of the proportionality constant, e.g. 0.43 for Al_5Fe_2, 0.39 for $Al_{13}Fe_4$ and 0.34 for the icosahedral Al-Fe phase.

3. Results and discussion

3.1. Fe-B

Glassy alloys are obtained close to the Fe-rich eutectic (17 at.% B) and the sequence of phases in the crystallization process is well established [26]. Calculated $\Delta\mu$ curves as a function of temperature for nucleation of bcc Fe, metastable Fe_3B and Fe_2B from an hypoeutectic $Fe_{85}B_{15}$ melt are shown in Fig. 1. The calculation has been performed using the assessment of [10]. $\Delta\mu$ is nil at the liquidus point and increases on undercooling. For bcc Fe, the curve is relatively insensitive to the shape of the liquid free energy and bends upwards because of the magnetic contribution to the crystal free energy. Using Equation 3, a straight line for $\Delta\mu$ is obtained with values only slightly higher than those obtained from the CALPHAD approach. For compounds, a downwards bending of $\Delta\mu$ occurs at low temperature as a consequence of the progressive change in shape of the liquid free energy curve caused by the excess specific heat. It is apparent that Equation 3 would give a straight line and, therefore, cannot be applied to intermetallic compounds. $\Delta\mu$ for the bcc phase is definitely the highest at low temperature. The behaviour of $\Delta\mu$ as a function of composition at the temperature of 800 K (close to the glass transition temperature) is given in Fig. 2. Depending on composition, the highest values pertain to either the bcc phase or Fe_2B, whereas those for metastable Fe_3B are always relatively lower.

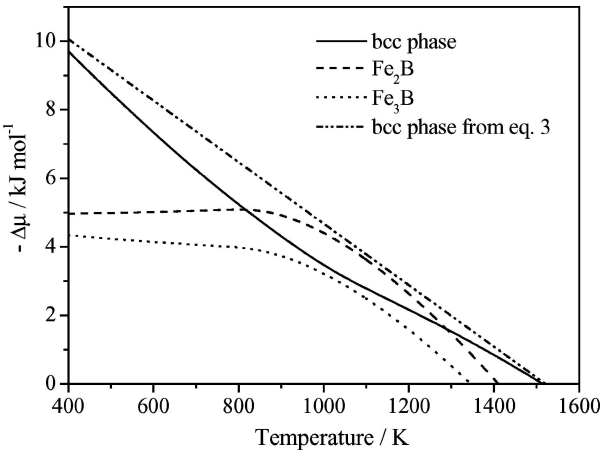

Figure 1 Fe-B system. Calculated difference of the chemical potentials between the various nucleating crystalline phases and the liquid-amorphous matrix ($\Delta\mu$) as a function of temperature for a $Fe_{85}B_{15}$ alloy. The calculated curve for the bcc phase according to Equation 3 is also reported (dashed dotted line).

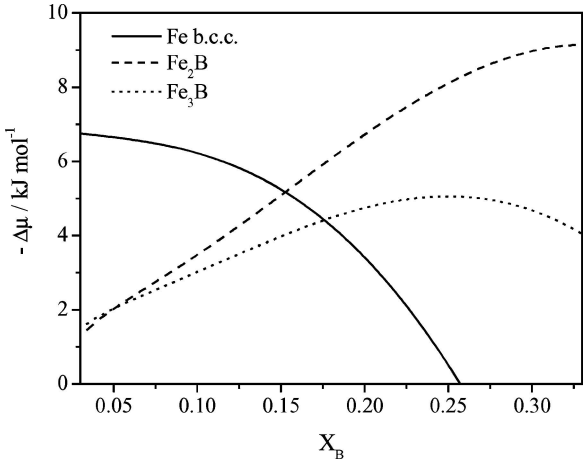

Figure 2 Fe-B system. Calculated difference of the chemical potentials between the various nucleating crystalline phases and the liquid-amorphous matrix ($\Delta\mu$) as a function of composition at a constant $T = 800$ K.

Values for the solid-liquid interfacial energy for all crystalline phases calculated according to Equations 4–6 at the melting temperature are reported in Table I. They have been obtained from optimised enthalpies of melting (ΔH_m) using $\alpha = 0.44$. The values obtained with Equations 4 and 5 are slightly different from those obtained with Equation 6 but all fall within the normal scatter of experimental data for γ_{SL} [13].

The driving force for nucleation (ΔG^*) has been computed with Equation 2 and is shown in Fig. 3a for $Fe_{85}B_{15}$. On approaching the melting temperature of each phase the driving force diverges because $\Delta\mu$ tends to zero and the nucleation frequency becomes negligible. On the contrary, at high undercooling ΔG^* for the bcc phase is the lowest at every temperature for an hypoeutectic composition, suggesting that its nucleation is always favoured. Using Equations 5 and 6 for the temperature dependence of the interfacial energy, all values of ΔG^* are reduced but the hierarchy of the various phases is not modified (Fig. 3b and c).

ΔG^* has then been calculated at 800 K according to Equations 4–6 (Fig. 4a–c) as a function of composition. In the Fe-rich side, the bcc phase has the highest tendency to nucleate, then there is a composition range where metastable Fe_3B should form first and finally for higher B content nucleation of Fe_2B is favoured. The decrease of γ_{SL} with undercooling produces a general reduction in the calculated values of the driving forces and a restriction of the field where Fe_3B should nucleate first. The range of composition where the driving force

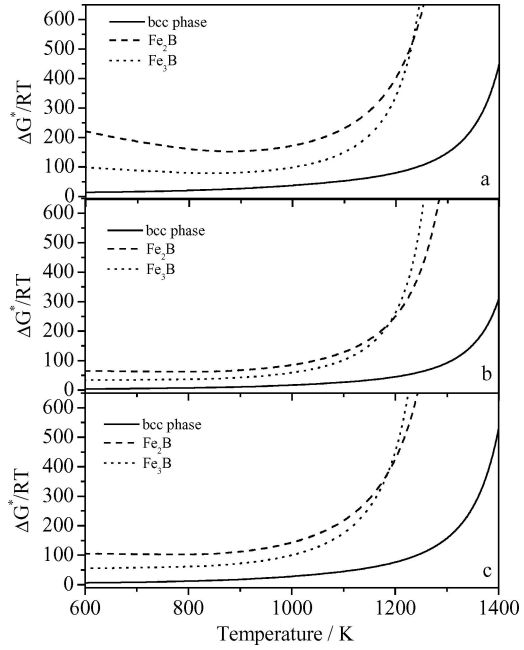

Figure 3 Fe-B system. Calculated driving forces for nucleation (ΔG^*) of various crystalline phases from a $Fe_{85}B_{15}$ melt as a function of temperature according to different models for the interfacial energy: (a) γ_{SL} from Equation 4; (b) γ_{SL} from Equation 5; (c) γ_{SL} from Equation 6.

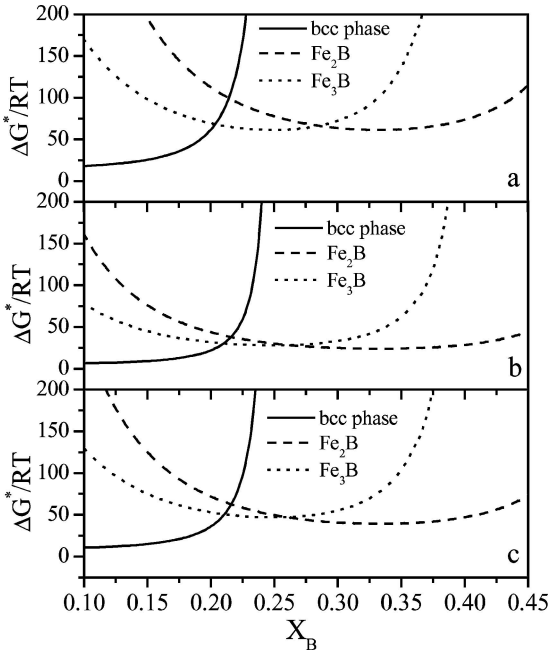

Figure 4 Fe-B system. Calculated driving forces for nucleation (ΔG^*) of various crystalline phases as a function of composition at constant $T = 800$ K according to different models for the interfacial energy: (a) γ_{SL} from Equation 4; (b) γ_{SL} from Equation 5; (c) γ_{SL} from Equation 6.

TABLE I Fe-B system. Computed values of the enthalpy of melting (ΔH_m) and interfacial energy ($\gamma(T_m)$) at the melting temperature T_m for various phases. Enthalpies have been obtained from the assessment in [10], interfacial energies by applying (a) Equation 4 or Equation 5 ($\alpha = 0.44$) or (b) Equation 6

Fe-B	Fe (bcc)	Fe_2B	Fe_3B
ΔH_m (kJ/mol)	13.81	26.89	18.11
T_m (K)	1811	1671	1431
$\gamma(T_m)^a$ (J/m^2)	0.155	0.302	0.203
$\gamma(T_m)^b$ (J/m^2)	0.187	0.364	0.245

for nucleation of crystalline phases is low corresponds fairly well to the range where amorphous phases can be obtained by rapid solidification [27]. Furthermore, Fig. 4 is also useful for understanding the sequence of phases obtained in devitrification [26]. From dynamic temperature X-ray diffraction the first appearance of the bcc phase was reported for B content up to about 17.5%, then metastable Fe_3B is found to form first. Results in Fig. 4 correctly predict the formation of Fe_3B, even if the range of first nucleation of the bcc phase is

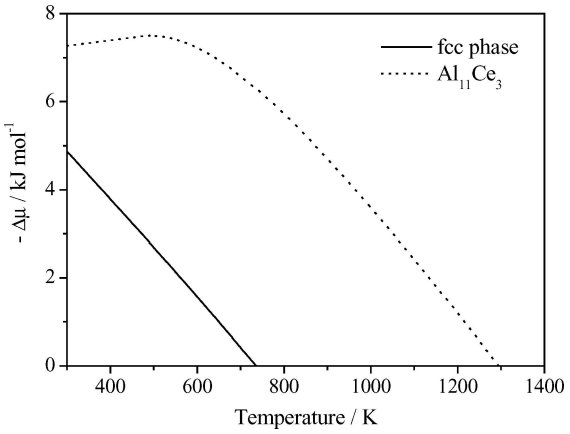

Figure 5 Al-Ce system. Calculated difference of the chemical potentials between the various nucleating crystalline phases and the liquid-amorphous matrix ($\Delta\mu$) as a function of temperature for a $Al_{91}Ce_9$ alloy.

overestimated. The agreement with the phase sequence found in devitrification and solidification shows that, even if heterogeneous nucleation can occur, it does not change the hierarchy of driving forces.

3.2. Al-Ce

The same approach hereto described for the Fe-B system has been applied to the Al-Ce glass forming system which is significant for the family of Al-rich glassy alloys containing a rare earth element [6]. Calculations have been performed for fcc Al and $Al_{11}Ce_3$ phases, which compete in devitrification in the Al-rich corner, using the CALPHAD assessment reported in [2]. Calculated curves of $\Delta\mu$ as a function of undercooling for a eutectic $Al_{91}Ce_9$ alloy (Fig. 5) show a similar behaviour with respect to the Fe-B system, with the bending for the compound at low temperature. In this case the lowest value is obtained for the Al phase which should then nucleate less likely then $Al_{11}Ce_3$.

Melting enthalpies and interfacial energies are reported in Table II. The calculated curves of the driving force for nucleation are shown in Fig. 6 as a function of composition at the temperature of 500 K. There is an increase in ΔG^* in agreement with the experimentally reported amorphisation range (7–10 at%Ce in [6]).

3.3. Al-Mn

In order to apply the foregoing method to nucleation of quasicrystals, a CALPHAD assessment of the system

TABLE II Al-Ce system. Computed values of the enthalpy of melting (ΔH_m) and interfacial energy ($\gamma(T_m)$) at the melting temperature T_m for various phases. Enthalpies have been obtained from the assessment in [2], interfacial energies by applying (a) Equations 4–5 ($\alpha = 0.44$) or (b) Equation 6

Al-Ce	Al (fcc)	$Al_{11}Ce_3$
ΔH_m (kJ/mol)	10.71	20.87
T_m (K)	933	1525
$\gamma(T_m)^a$ (J/m^2)	0.120	0.234
$\gamma(T_m)^b$ (J/m^2)	0.145	0.282

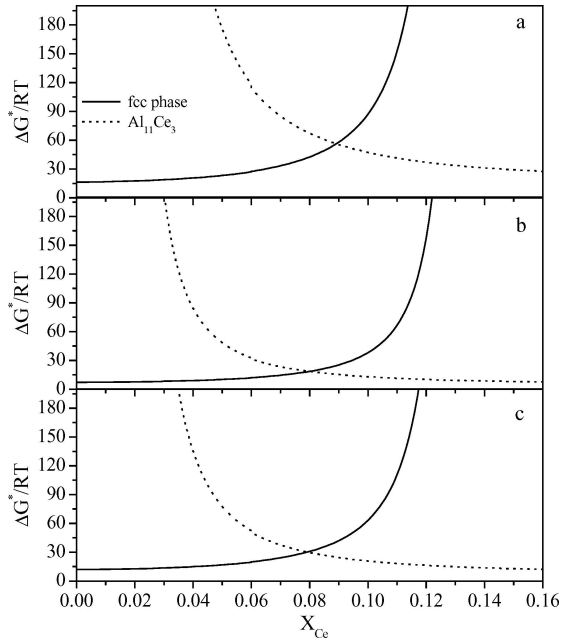

Figure 6 Al-Ce system. Calculated driving forces for nucleation (ΔG^*) of fcc and $Al_{11}Ce_3$ phases as a function of composition at constant $T = 500$ K according to different models for the interfacial energy: (a) γ_{SL} from Equation 4; (b) γ_{SL} from Equation 5; (c) γ_{SL} from Equation 6.

including the Gibbs energy of the icosahedral phase is required. However, none has been reported in the literature. A recent assessment ([11]) has then been used to derive its Gibbs free energy as a difference from either the equilibrium crystal phases or the liquid free energy employing data on heats of transformation according to [28].

The calculated $\Delta\mu$ curves for various phases which compete with quasicrystals formation in rapid

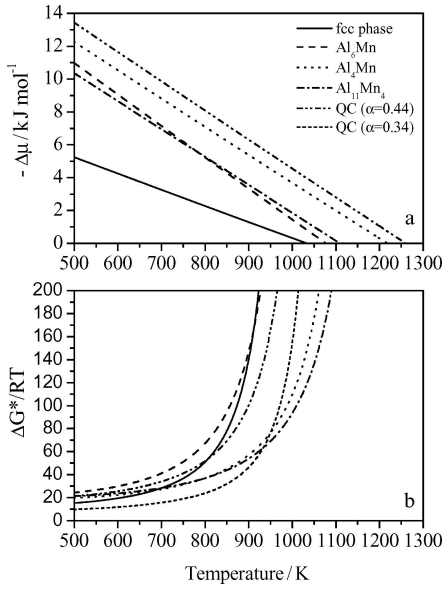

Figure 7 Al-Mn system. (a) Calculated difference of the chemical potentials between the various nucleating phases and the liquid-amorphous matrix ($\Delta\mu$) as a function of temperature for a $Al_{80}Mn_{20}$ composition. (b) Calculated driving forces for nucleation (ΔG^*) of various phases from a $Al_{80}Mn_{20}$ composition as a function of temperature. Equation 4 has been used for the interfacial energy, but two values of α have been used for quasicrystals: dash double dot line, $\alpha = 0.44$; short dash dot, $\alpha = 0.34$.

TABLE III Al-Mn system. Computed values of the enthalpy of melting (ΔH_m) and interfacial energy ($\gamma(T_m)$) at the melting temperature T_m for various phases. Enthalpies have been obtained from the assessment in [11], interfacial energies by applying (a) Equations 4–5 ($\alpha = 0.44$) or (b) Equation 6

Al-Mn	Al	Al_6Mn	Al_4Mn	$Al_{11}Mn_4$	Icosahedral phase
ΔH_m (kJ/mol)	10.71	20.46	20.54	22.41	18.84
T_m (K)	933	1090	1218	1277	1110
$\gamma(T_m)^a$ (J/m^2)	0.120	0.229	0.230	0.252	0.187
$\gamma(T_m)^b$ (J/m^2)	0.145	0.277	0.278	0.303	0.255

solidification are shown in Fig. 7a for a $Al_{80}Mn_{20}$ melt. The linear behaviour is due to the simpler model used for the liquid phase which does not include any term to account for excess specific heat contributions. $\Delta\mu$ values for the icosahedral phase are intermediate between those for intermetallic compounds and the lower value of the fcc phase. The calculation of interfacial energies has been performed with the same approach as for the other systems (Table III). The driving forces for nucleation are shown in Fig. 7b where the nucleation of quasicrystals does never appear the most probable. The temperature dependence of the interfacial energy expressed by Equations 5 and 6 does not significantly modify this result. It is apparent that the correct hierarchy in phase nucleation can be reproduced only by lowering the value of γ_{SL}, e.g. in terms of Equation 4 by reducing the value of the α constant below 0.44. Following the suggestion of [14] for the icosahedral phase in Al-Fe, α is taken as 0.34 also for Al-Mn (Fig. 7b). The resulting ΔG^* curve correctly predicts a high tendency to nucleation for quasicrystals on undercooling, according to experimental findings. The low value of the liquid-crystal interfacial free energy is consistent with the similarity in short range order of the liquid and icosahedral phases recently demonstrated by means of various diffraction experiments [29, 30].

4. Conclusions

The use of experimentally assessed CALPHAD models and optimised thermodynamic functions has proved useful in evaluating the driving forces for nucleation. Care must be used in considering also metastable phases in the simulation. With simple formulae for the solid-liquid interfacial energy, including a temperature dependence, driving forces for nucleation are computed which explain well experimentally determined phase selection and amorphous ranges in Fe-B and Al-Ce. In the case of Al-Mn, however, a different proportionality constant is needed to allow for nucleation of quasicrystals.

Acknowledgements

Studies on thermophysical properties of alloys are supported by ESA-ESTEC Contract n. 14306/01/NL/SH-MAP Project N. AO-99-022 "Thermolab" and ASI Contract n. I/R/073/01.

References

1. J. W. CHRISTIAN, "The Theory of Transformations in Metals and Alloys," 1st ed., (Pergamon Press, Oxford, 1965) p. 537.
2. M. BARICCO, F. GAERTNER, G. CACCIAMANI, P. RIZZI, L. BATTEZZATI and A. L. GREER, *Mater. Sci. Forum* **269–272** (1998) 553.
3. N. SAUNDERS and A. P. MIODOWNIK, "CALPHAD, A Comprehensive Guide," edited by R. W. Cahn (Pergamon, 1998).
4. T. IIDA and R. I. L. GUTHRIE, "The Physical Properties of Liquid Metals" (Clarendon Press, Oxford Science Publications, 1993).
5. A. INOUE, "Bulk Amorphous Alloys, Materials Science Foundations," edited by M. Magini and F. H. Wohlbier (Trans Tech Publications, Ueticon-Zuerich, Switzerland, 1998) Vol. 4, p. 1.
6. A. INOUE, *Progr. Mater. Sci.* **43** (1998) 365.
7. A. ZHU, S. J. POON and G. J. SHIFLET, *Scripta Materialia* **50** (2004) 1451.
8. K. F. KELTON, *J. Non-Cryst. Solids* **334/335** (2004) 253.
9. D. SHECHTMAN, I. BLECH, D. GRATIAS and J. W. CAHN, *Phys. Rev. Lett.* **53** (1984) 1951.
10. M. PALUMBO, G. CACCIAMANI, E. BOSCO and M. BARICCO, *Intermetallics* **11** (2003) 1293.
11. A. JANSSON, in "COST 507 Thermochemical Database for Light Metal Alloys," edited by I. Ansara, A. T. Dinsdale and M. H. Rand (1998) Vol. 2.
12. M. PALUMBO, E. BOSCO, G. CACCIAMANI and M. BARICCO, *CALPHAD* **25** (2001) 625.
13. N. EUSTATHOPOULOS, *Intern. Metal Rev.* **28** (1983) 189.
14. D. HOLLAND-MORITZ, *Intern. J. Non-Equilibr. Proc.* **11** (1998) 169.
15. C. V. THOMPSON and F. SPAEPEN, *Acta Met.* **31** (1983) 2021.
16. L. BATTEZZATI, *Mater. Sci. Engng.* **A304–306** (2001) 103.
17. *Idem*, *ibid.* **A178** (1994) 43.
18. F. SOMMER, *ibid.* **A178** (1994) 49.
19. J. O. ANDERSSON, T. HELANDER, L. HOGLUND, P. SHI and B. SUNDMAN, *CALPHAD* **26** (2002) 273.
20. D. TURNBULL and R. E. CECH, *J. Appl. Phys.* **21** (1950) 804.
21. K. F. KELTON, Crystal Nucleation in Liquids and Glasses, in "Solid state physics. Advances in Research and Applications" (Academic Press, New York, 1991) Vol. 45, p. 75.
22. J. L. WALKER, as quoted in B. Chalmers, "Principles of Solidification," (John Wiley and Sons, New York, 1964) p. 77.
23. L. GRANASY, *J. Non-Cryst. Solids* **162** (1993) 301.
24. F. SPAEPEN, Homogeneous Nucleation and the Temperature Dependence of the Crystal-Melt Interfacial Tension, in "Solid State Physics," edited by H. Ehrenreich and D. Turnbull (Academic Press, New York, 1994) Vol. 47, p. 1.
25. L. BATTEZZATI and A. CASTELLERO, in "Nucleation and the Properties of Undercooled Melts, Materials Science Foundations," edited by M. Magini and F. H. Wohlbier (Trans Tech Publications Ltd., Uetikon-Zurich, Switzerland, 2002) Vol. 15, p. 1.
26. Y. KAHN, E. KNELLER, M. SOSTARICH and Z. METALLKD, **72** (1981) 553.
27. C. ANTONIONE, L. BATTEZZATI, G. COCCO and F. MARINO, *Z. Metallkde* **75** (1984) 714.
28. L. BATTEZZATI, C. ANTONIONE and F. MARINO, *J. Mater. Sci.* **24** (1989) 2324.
29. D. HOLLAND-MORITZ, "Short-Range Order in Undercooled Metallic Liquids, Presented at RQ11 Conference, Oxford, England, August 2002.
30. K. F. KELTON, Ti/Zr/Hf Based Quasicrystals, Presented at RQ11 Conference, Oxford, England, August 2002.

Received 31 March
and accepted 20 October 2004